DOI: 10.1002/cmdc.200700103

Designed Amyloid β Peptide Fibril—A Tool for High-Throughput Screening of Fibril Inhibitors

Gunnar T. Dolphin, Myriam Ouberai, Pascal Dumy,* and Julian Garcia*[a]

Amyloid β peptide (Aβ) fibril formation is widely believed to be the causative event of Alzheimer's disease pathogenesis. Therapeutic approaches are therefore in development that target various sites in the production and aggregation of Aβ. Herein we present a high-throughput screening tool to generate novel hit compounds that block Aβ fibril formation. This tool is an application for our fibril model ($A\beta_{16-37}Y_{20}K_{22}K_{24})_4$, which is a covalent assembly of four Aβ fragments. With this tool, screening studies are complete within one hour, as opposed to days with native $A\beta_{1-40}$. A Z′ factor of 0.84 ± 0.03 was determined for fibril formation and inhibition, followed by the reporter molecule thioflavin T. Herein we also describe the analysis of a broad range of reported inhibitors and non-inhibitors of Aβ fibril formation to test the validity of the system.

Introduction

Amyloid diseases are protein-misfolding disorders characterized by aggregation of proteins and peptides, which form insoluble fibrils in vivo that accumulate into amyloid plaques. The most common forms of amyloid disease are the neurodegenerative disorders Alzheimer's, Parkinson's, and Huntington's diseases.[1–3] Even though amyloid-forming proteins show little sequence homology, amyloid fibrils share common characteristics, such as unbranched fibrillar morphology, cross-β-sheet structure, and binding of the amyloid-specific dyes Congo red and thioflavin T (ThT).

Alzheimer's disease (AD) is a progressive degenerative disease characterized by amyloid fibrillar deposits in the brain that consist mainly of the amyloid β peptides $A\beta_{1-40}$ and $A\beta_{1-42}$.[4] Amyloid β peptides are proteolytic fragments of the amyloid precursor protein[5] and include a membrane segment, giving them their highly hydrophobic and aggregation-prone nature. Aβ is normally present as a random coil, but through formation of intermediate oligomers, misfolds into fibrils, and further aggregation of the fibril forms amyloid. The mechanism for amyloid formation is suggested to occur through a nucleation-dependent polymerization.[6,7]

It is widely accepted that the formation of fibrils is implicated in the neurotoxicity associated with AD, but there is still much discussion about which aggregation state of Aβ is toxic and what the mechanisms of toxicity are. In AD patients both the disruption of cellular calcium homeostasis and increased oxidative stress have been observed.[8] Suggested mechanisms for the observed toxicity in AD include Aβ interaction with neuron membranes, generating an increase in intracellular calcium concentration.[9] This has been proposed to occur through either insertion of Aβ in the cellular membrane with formation of pores,[10,11] or through direct interaction of Aβ with membranes, which leads to their instability.[12–14] Moreover, elevated intracellular Ca^{2+} levels can trigger excessive phosphorylation of tau protein, a major component of paired helical filaments, which leads to the accumulation of neurofibrillary tangles, a typical pathology of AD and related diseases.[15] Oxidative damage observed in the brains of AD patients has been suggested to be a result of Aβ-mediated reduction of Cu^{2+} and Fe^{3+}, leading to the production of reactive oxygen species (ROS).[16,17] The ROS, in turn, modify and decrease the function of critical enzymes in energy metabolism.[18]

To date, there is no detailed structural information about amyloid fibrils, owing to short-lived intermediates and their insoluble nature. From experiments using circular dichroism (CD), solid-state NMR, EPR, and X-ray scattering, amyloid fibrils have been determined to contain a high amount of β-sheet structure. Key features of Aβ organization in fibrils have also been revealed, such as the cross-β-sheet structural motif, where β strands are perpendicular to the fibril axis and form intermolecular parallel β sheets extending the length of the fibril.[19]

A number of therapeutic approaches are in development that target different sites on the pathway towards Alzheimer's disease. As fibril formation of Aβ is implicated in AD pathogenesis, important strategies include: decreasing Aβ production,[20] stimulating the immune system to remove Aβ from the brain,[21] and direct inhibition of the Aβ self-assembly process.[22,23] For the suppression or prevention of the transition from monomeric to oligomeric and polymeric Aβ species, an accumulation of reports that describe small-molecule inhibitors has emerged in the past few years. This approach was initially

[a] *Dr. G. T. Dolphin, M. Ouberai, Prof. P. Dumy, Prof. J. Garcia*
Département Chimie Moléculaire (DCM), UMR 5250, ICMG-FR
Université Joseph Fourier, BP 53, 38041 Grenoble Cedex 9 (France)
Fax: (+33) 476514946
E-mail: julian.garcia@ujf-grenoble.fr
pascal.dumy@ujf-grenoble.fr

Supporting information for this article is available on the WWW under http://www.chemmedchem.org or from the author.

based on the finding that the small dye, Congo red, interacts specifically with amyloid fibrils and inhibits their formation.[24]

ThT also shows specific binding to amyloid, and is the simplest way to identify amyloid structures and to follow their formation and disassembly in the search for inhibitor compounds. ThT is highly specific and sensitive for the characteristic cross-β-sheet structure of amyloid fibrils, and its binding is easily followed by fluorescence spectroscopy. This is due to a large excitation spectral red shift (bathochrome shift), which allows selective excitation of bound ThT.[25] ThT binding can be followed by studying aliquots of amyloid fibril mixtures added to a solution of ThT or by addition of ThT to the fibril-forming mixtures, as it has been shown to have little effect on the assembly process.[26,27]

However, the discovery of inhibitors is hampered by the rather slow phases of nucleation and self assembly of Aβ peptides, which has been described as a nucleation-dependent polymerization mechanism.[6,7] The nucleation and lag phases usually take a few days, and the whole process to fully formed fibrils can take more than a week. However, the nucleation phase can be avoided by the addition of preformed fibrils that seed the self association. The kinetic processes involved in Aβ organization are highly variable; identical kinetics studies can show different lag phases. For these reasons, there is a need for a fast and reproducible screening tool for the search of amyloid inhibitors. This tool should have the properties of easy handling and stability and should be adaptable to automatic analysis.

Herein we present an application for the engineered fibril building block, $(A\beta_{16-37}Y_{20}K_{22}K_{24})_4$, as a high-throughput screening tool for amyloid inhibitors. Previously we reported the preparation and characterization of $(A\beta_{16-37}Y_{20}K_{22}K_{24})_4$, a fourfold assembly of Aβ fragments attached to a template scaffold (Figure 1).[28] We demonstrated the formation of well-formed fibrils with this assembly by transmission electron microscopy (TEM), CD, and binding with the dyes ThT and Congo red. This construct also displayed important characteristics for high-throughput screening such as highly controllable kinetics of fibril formation, and as the formation of fibrils is rapid and occurs without a lag phase, oligomer formation is expected not to occur with this system. We also demonstrated control over both the initiation and the kinetics of fibril formation by the addition of HPO_4^{2-} at various concentrations.[28] As no formation of fibrils occurred with monovalent anions, we concluded that the formation of fibrils is due to charge neutralization of the net positively charged assembly with dianions such as HPO_4^{2-}.

We report herein a reproducible analysis of fibril formation and inhibition with amyloid inhibitors, following the real-time change of fluorescence in ThT–fibril interactions. The studies are performed on microplates and the kinetics are fast and complete within one hour. The formation of fibrils is started by simply adding HPO_4^{2-} to solutions of $(A\beta_{16-37}Y_{20}K_{22}K_{24})_4$, ThT, and potential inhibitor molecules. No aggregation or fibril formation is observed without the addition of HPO_4^{2-}. To test the validity of our system, this study was carried out with a broad range of reported inhibitors and non-inhibitors.

Results

The screening tool

Previously we reported the preparation of the Aβ fibril building block, $(A\beta_{16-37}Y_{20}K_{22}K_{24})_4$, which is a fourfold assembly of Aβ fragments, residues 16–37 of full-length Aβ, attached to a template scaffold (Figure 1).[28] Furthermore, for increased solubility by a net positive charge, three mutations were introduced into the sequence that forms the hydrophilic surface of the filament, namely Phe 20 → Tyr, Glu 22 → Lys, and Val 24 → Lys. This fourfold assembly configuration thus creates two cross-sections (as compared with native Aβ fibrils), each containing two Aβ segments that fold through side-chain—side-chain hydrophobic interactions. The characteristic amyloid cross-β-sheet structure is formed between the cross-sections, and aggregation of assemblies forms fibrils (Figure 1). The structure was found to be highly soluble, and the cross-β-sheet structure and formation of fibrils were confirmed by CD, TEM, and specific binding of ThT and CR.[28]

Herein we present an application for the designed amyloid β peptide fibril building block, $(A\beta_{16-37}Y_{20}K_{22}K_{24})_4$, as a tool for high-throughput screening (HTS) of fibril inhibitors. Important characteristics for HTS applications are displayed in the folding and self association of $(A\beta_{16-37}Y_{20}K_{22}K_{24})_4$ such as rapid fibril formation and control over the initiation of fibril formation by the addition of the divalent anion HPO_4^{2-}. Also, the kinetics are highly sensitive to the HPO_4^{2-} concentration, which permits fine-tuning of the kinetics depending on instrumentation. The kinetics are easily followed by the binding of the cross-β-sheet-specific dye ThT (see Table 1 for structure). Figure 2a shows fluorescence spectra of ThT at various times after initiation of $(A\beta_{16-37}Y_{20}K_{22}K_{24})_4$ fibril formation with phosphate buffer (5 mM pH 7.1). In the study of the stagnant solution of ThT and its interaction with $(A\beta_{16-37}Y_{20}K_{22}K_{24})_4$, strong fluorescence intensity is observed at 480 nm, which increases as a function of fibril growth (Figure 2a). By

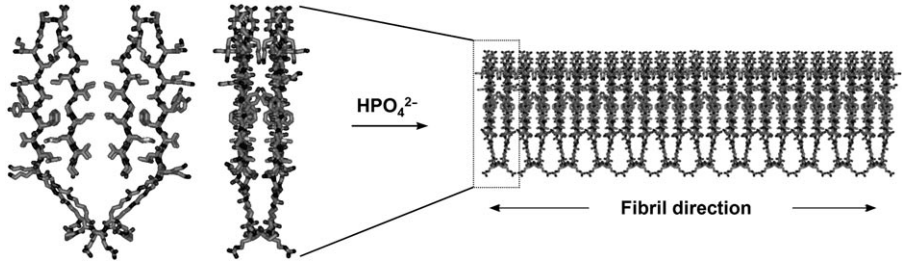

Figure 1. Modeled representation of the fibril building block $(A\beta_{16-37}Y_{20}K_{22}K_{24})_4$, viewed along and from the side of the fibril axis (left); self-assembled $(A\beta_{16-37}Y_{20}K_{22}K_{24})_4$ forms a fibril (represented at right).

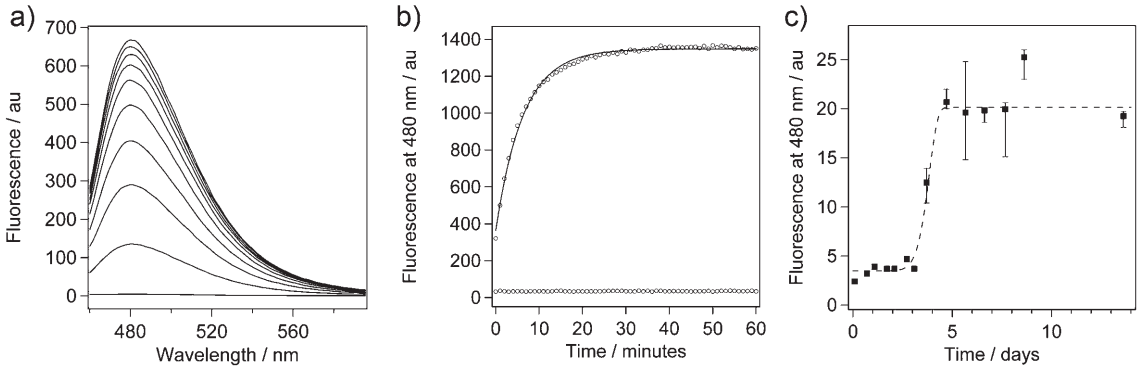

Figure 2. Comparison of folding kinetics between $(A\beta_{16-37}Y_{20}K_{22}K_{24})_4$ and $A\beta_{1-40}$. a) Fluorescence spectra of ThT (10 μM) in the presence of $(A\beta_{16-37}Y_{20}K_{22}K_{24})_4$ (4 μM) at various times after the addition of phosphate buffer (5 mM, pH 7.1, 20 °C). Spectra are plotted at (from the bottom) 0, 6, 15, 23, 32, 40, 48, 57, 75, and 84 min; $\lambda_{ex}=440$ nm. b) Folding kinetics of $(A\beta_{16-37}Y_{20}K_{22}K_{24})_4$ (70 μL, 4 μM, 25 °C) in 5 mM HPO_4^{2-} (data points at top), monitored by the fluorescence of bound ThT at 480 nm; the solid line is the exponential curve fit. Data points at bottom represent the absence of phosphate. c) Folding kinetics of $A\beta_{1-40}$ (50 μM) in phosphate buffer (50 mM) and NaCl (100 mM) pH 7.4 at 37 °C, monitored by ThT fluorescence at 480 nm with excitation at 440 nm. Data were obtained from 4-μL aliquots that were removed from the aggregation mixture and analyzed separately with 96 μL ThT (10 μM), HPO_4^{2-} (50 mM, pH 7.1; see Experimental Section). To aid the eye, the data are curve-fitted with an extended-exponential function (dashed line). Data in a) and c) were recorded in a 0.3 cm reduced cuvette; data in b) were recorded using a microplate reader.

studying the increase in fluorescence at 480 nm as a function of time (Figure 2b), it can be seen that the system shows folding with no lag phase and is complete within one hour. The kinetics data are well fitted to a single-exponential function, and the measured rate constant for the complete formation of folded fibrils is 0.2 min^{-1} at 25 °C.

For screening purposes, the obvious problem with native Aβ is its slow kinetics of fibril formation, which is shown for $A\beta_{1-40}$ in Figure 2c. As can be seen, the disadvantage is first due to a long nucleation phase (lag phase) that takes more than three days, and thereafter, the slow phase of self assembly into fibrils, as evident with the increase in ThT fluorescence. The whole process to fully formed fibrils is complete after about six days. The aggregation kinetics study of $A\beta_{1-40}$ (50 μM) was performed in stagnant solution under optimal conditions (50 mM HPO_4^{2-} and 100 mM NaCl, pH 7.4 at 37 °C). It is for this slow process of $A\beta_{1-40}$ fibril formation that we became interested in our Aβ fibril building block as a tool for HTS.

Screening studies

The validity of the present system was subjected to analysis with a broad range of reported inhibitors and non-inhibitors of native Aβ fibril formation. The library of inhibitors contained 19 compounds belonging to more than 10 different chemical classes (Table 1). Also, in the design of the inhibitor library we chose inhibitors that would create an array of previously reported inhibitory effects against $A\beta_{1-40}$ fibril formation. The compounds tested are not only well known to inhibit Aβ aggregation, but are also commercially available and range from natural products to synthetic dyes. Only a cholic acid modified Aβ fragment was prepared as previously reported.[29] Table 1 shows that a common feature for most of the reported amyloid inhibitors is the presence of aromatic groups, which are expected to interact with the aromatic residues commonly found in amyloid-forming peptides.[30]

The present system is easy to handle; inhibition studies of fibril formation are performed on microplates for multiple and automatic data collection. First a stock solution containing both the fibril-forming building block $(A\beta_{16-37}Y_{20}K_{22}K_{24})_4$ and the fluorescent reporter ThT was added to the required wells. Potential inhibitors were then added, and the formation of fibrils was started by the addition of phosphate buffer (HPO_4^{2-}). The final concentrations used were 4 μM $(A\beta_{16-37}Y_{20}K_{22}K_{24})_4$, 10 μM ThT, and 5 mM HPO_4^{2-}. The concentrations of studied inhibitors were 0, 0.01, 0.1, 1, 10, and 100 μM. No aggregation or fibril formation was observed without the addition of HPO_4^{2-} (Figure 2b). The kinetics were performed at room temperature and monitored by the fluorescence of fibril-bound ThT ($\lambda_{ex}=$ 440 nm, $\lambda_{em}=480$ nm) as a function of time at 1-min intervals. All inhibitor compounds were analyzed in the absence of $(A\beta_{16-37}Y_{20}K_{22}K_{24})_4$ and ThT by UV to exclude the possibility that they act as potential inner filters of ThT at the excitation or emission wavelengths, thus acting as false positives. From this analysis we found that only the compounds curcumin, methyl yellow, chlorazol black E, and rifampicin have absorbencies near one or both of the excitation/emission wavelengths. For these four compounds we therefore expect that, to some degree, the fluorescence decrease observed at high compound concentration is due to an absorbency filtration effect (see Discussion Section below).

As the compounds display various degrees of inhibitory effects, we grouped them according to their effects towards $(A\beta_{16-37}Y_{20}K_{22}K_{24})_4$ fibril formation, to give representative results with a compound from each group (Figure 3). The five groups formed are classified as: very strong inhibitors ($IC_{50}<1$ μM), strong inhibitors ($IC_{50}=1$–10 μM), medium inhibitors ($IC_{50}=10$–100 μM), weak inhibitors ($IC_{50}\sim100$ μM), and non-inhibitors ($IC_{50}>100$ μM). Almost all inhibitors tested, as previously reported for $A\beta_{1-40}$, inhibit the aggregation of $(A\beta_{16-37}Y_{20}K_{22}K_{24})_4$ in a dose-dependent fashion; only one, α-lipoic acid, did not

Table 1. Thioflavin T and compounds used for inhibition studies of $(A\beta_{16-37}Y_{20}K_{22}K_{24})_4$ fibril formation.

Compd class	Compd	Structure	Compd class	Compd	Structure
anthracycline	tetracycline	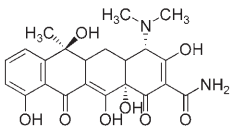	porphyrin	hemin chloride	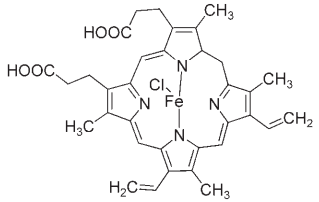
benzothiazoles	thioflavin T	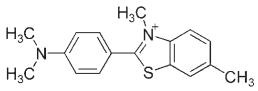	sulfonated dye	chlorazol black E	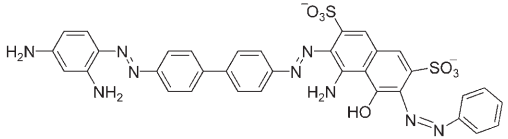
	basic blue 41	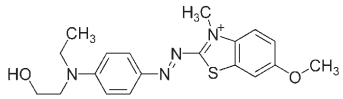	rifamycin	rifampicin	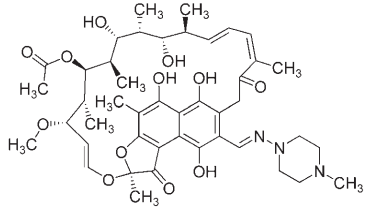
modified Aβ fragment	cholyl-LVFFA	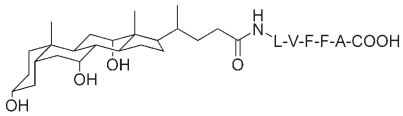	other	2-amino-4-chlorophenol	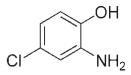
phenothiazine	thionin	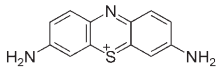		methyl yellow	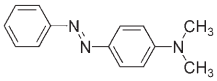
polyphenoles	curcumin	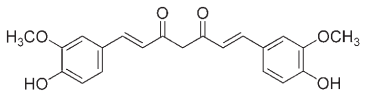		α-lipoic acid	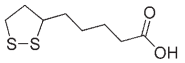
	NDGA	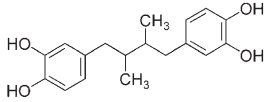		nicotine	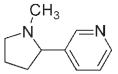
	myricetin	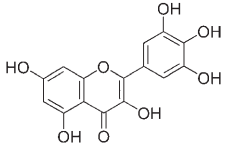		pyridine	
	4,4′-dihydroxybenzophenone	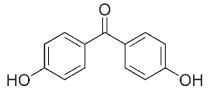	camphor	camphorsulfonic acid	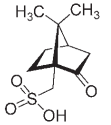
	dopamine	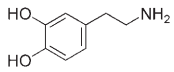	cyclodextrin	β-cyclodextrin	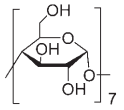

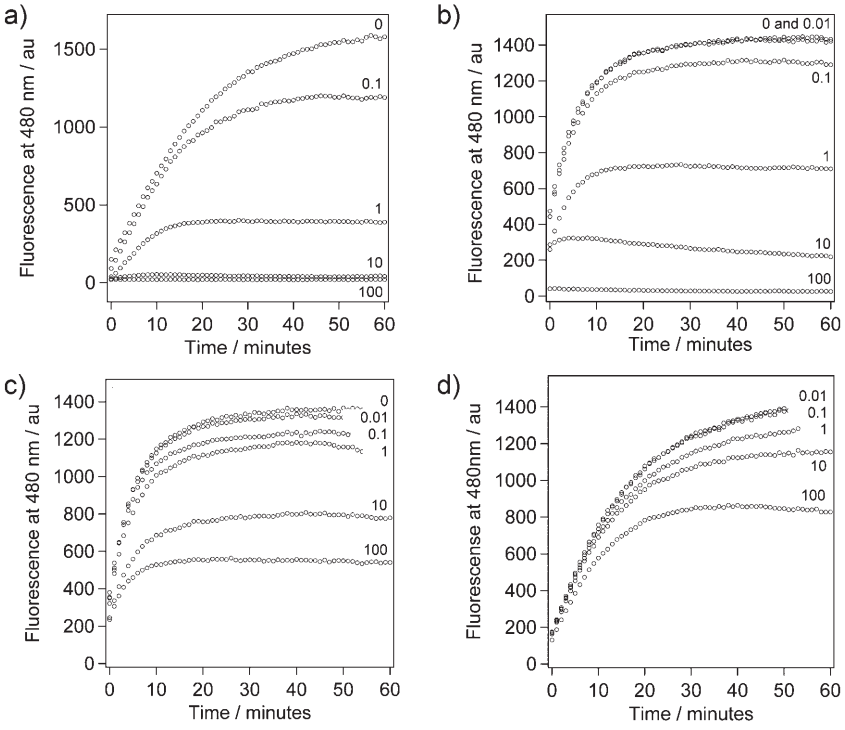

Figure 3. Representative inhibition data for selected inhibitors of $(A\beta_{16-37}Y_{20}K_{22}K_{24})_4$ fibril formation: a) myricetin, b) NDGA, c) tetracycline, and d) 2-amino-4-chlorophenol. All inhibition studies were monitored by the fluorescence of bound ThT (10 μM; $\lambda_{ex}=440$ nm, $\lambda_{em}=480$ nm) to $(A\beta_{16-37}Y_{20}K_{22}K_{24})_4$ (4 μM) in HPO_4^{2-} (5 mM, pH 7.1) at room temperature. Respective inhibitor concentrations (μM) are indicated next to each curve.

display a strong inhibitory effect as previously reported (see below).

Very strong inhibitors

The group of very strong inhibitors is formed by the compounds basic blue 41, the yellow curry pigment curcumin, methyl yellow, the wine-related polyphenol myricetin, and thionin (Table 2). Figure 3a shows representative results for this group, with those of myricetin. Co-incubation of $(A\beta_{16-37}Y_{20}K_{22}K_{24})_4$ with myricetin markedly decreased the formation of amyloid fibrils as detected by the specific binding of ThT in comparison with the control without inhibitor. Increasing the concentration of these inhibitors progressively reduced the signal from ThT in a dose-dependent fashion. For this group, the presence of 10 μM or more of the inhibitor compounds completely blocked the aggregation of $(A\beta_{16-37}Y_{20}K_{22}K_{24})_4$, and in the presence of inhibitor at 1 μM, the signal from ThT was decreased by more than 75%. The concentrations for inhibiting the aggregation of $(A\beta_{16-37}Y_{20}K_{22}K_{24})_4$ by 50% (IC_{50} values) for these compounds are listed in Table 2. Comparing the IC_{50} values obtained from this group of inhibitors with the system reported herein with those previously reported towards $A\beta_{1-40}$, a high degree of correlation is observed. The IC_{50} values reported for this group are between 0.2 and 0.4 μM, and previously reported values for $A\beta_{1-40}$ are between 0.3 and 1.5 μM (see Table 2 for references).

Strong inhibitors

A large decrease in ThT fluorescence was also observed in the presence of compounds that we grouped as strong inhibitors: chlorazol black E, hemin chloride, nordihydroguaiaretic acid (NDGA), and rifampicin. Figure 3b shows representative results for this group with the data from NDGA. Similar to the very strong inhibitors, a progressive increase in the concentration of these inhibitors reduced the signal from ThT in a dose-dependent fashion. For this group, complete reduction of the aggregation of $(A\beta_{16-37}Y_{20}K_{22}K_{24})_4$ is observed only in the presence of inhibitor at 100 μM. At 10 μM, a small amount of fibril formation can be seen, and at 1 μM, the signal from ThT is decreased to ~50%. Table 2 shows the IC_{50} values determined for the group of strong inhibitors. They are between 0.9 and 1.4 μM and thus show good correlation with the corresponding values that were previously reported for $A\beta_{1-40}$, which lie between 0.1 and 6 μM.

Medium inhibitors

The group of medium inhibitors includes tetracycline and cholyl-LVFFA. Cholyl-LVFFA is a cholic acid modified amino terminus of an Aβ fragment consisting of residues 17–21. Both of these inhibitors reduced the signal from ThT in a dose-dependent fashion (Figure 3c). In this case, complete inhibition of the aggregation of $(A\beta_{16-37}Y_{20}K_{22}K_{24})_4$ is not observed in the concentration range studied. The IC_{50} values are 10 μM for cholyl-LVFFA and 35 μM for tetracycline. These data are in good agreement with the corresponding values previously reported: <5 μM for cholyl-LVFFA and 50 μM for tetracycline (see Table 2).

Weak inhibitors

A relatively small decrease in ThT fluorescence was observed in the presence of compounds we classified as weak inhibitors: 2-amino-4-chlorophenol and 4,4′-dihydroxybenzophenone (Figure 3d). For this group, a concentration of about 100 μM, the highest concentration studied, is required to reduce the ThT signal to 50% of that observed without inhibitor. The IC_{50} value of 100 μM for 2-amino-4-chlorophenol is about the same as that previously reported ($IC_{50}=30$ μM, Table 2). Published data for $A\beta_{1-40}$ inhibition by 4,4′-dihydroxybenzophenone was

not found. However, a study of the closely related 2,2′-dihydroxybenzophenone was reported, with an IC_{50} value of >40 μM,[31] indicating that it is also a weak inhibitor or a non-inhibitor.

Non-inhibitors

The group of non-inhibitors is composed of the lipid-soluble antioxidant α-lipoic acid, β-cyclodextrin, camphorsulfonic acid, the anti-Parkinson's agent dopamine, nicotine, and pyridine (Table 2). Figure 4 shows the results of co-incubation of $(A\beta_{16-37}Y_{20}K_{22}K_{24})_4$ with these compounds, and here it is clear that they exert only small effects on the specific binding of ThT. Nicotine was previously reported to show anti-fibril-forming effects on $A\beta_{1-40}$ at relatively high concentrations ($IC_{50}=10$ mM).[42] In the same report it was also shown that pyridine had no inhibitory effect on fibril formation with $A\beta_{1-40}$, and thus our results for pyridine and nicotine correlate well with those previously reported. Camphorsulfonic acid and β-cyclodextrin have a nonaromatic structure that is atypical for fibril inhibitors and were tested here as non-inhibitor controls. Both of these compounds gave the expected results, showing no inhibition at 100 μM (Figure 4a).

We did not detect inhibitory effects using the current system with the inhibitors recently reported by Yamada and co-workers: α-lipoic acid[39] and dopamine[40] (Figure 4b,c). They reported IC_{50} values for inhibition of $A\beta_{1-40}$ fibril formation of 3.2 μM for α-lipoic acid and 0.01 μM for dopamine. Their results for dopamine show a very strong inhibitory effect, making it one of the strongest reported inhibitors to date. However, the research group of Fink reported a weak inhibitory effect of dopamine, which was required at 10–100 μM to inhibit the formation of amyloid fibrils from a solution of $A\beta_{1-40}$ (230 μM in 25 mM Tris, 100 mM NaCl, pH 7.5, 37 °C).[41] Owing to this controversy with dopamine we set out to reproduce the previously reported results on the inhibition of $A\beta_{1-40}$ fibril formation with both α-lipoic acid and dopamine. The inhibition study of $A\beta_{1-40}$ (50 μM) was performed in stagnant solution using the same conditions as reported by Yamada's research group: HPO_4^{2-} (50 mM, pH 7.4) and NaCl (100 mM) at 37 °C.[39,40] We co-incubated $A\beta_{1-40}$ with the inhibitors at 0, 1, 10, and 100 μM, and aliquots were studied for changes in ThT fluorescence. As apparent in Figure 5, and as is also the case for the $(A\beta_{16-37}Y_{20}K_{22}K_{24})_4$ system, we did not observe the expected inhibition as previously reported. In our studies we observe fibril formation at all α-lipoic acid concentrations tested ($IC_{50}>100$ μM), and for dopamine we observed inhibition only at 100 μM (IC_{50}: 10–100 μM), similar to that reported by Fink and co-workers.[41] In our hands both α-lipoic acid and dopamine can be classified as weak or non-inhibitors of $(A\beta_{16-37}Y_{20}K_{22}K_{24})_4$ and $A\beta_{1-40}$ fibril formation.

To assess the quality (precision) and suitability of the fibril inhibitor assay for HTS, the *Z′* factor was determined for the system with and without inhibitor in 96-well plates (Figure 6). Assays with a *Z′* factor value between 0.5 and the maximum value of 1 are suitable for HTS. Using the inhibitor curcumin at 100 μM and our fibril model at 5 μM, the *Z′* factor was calculated as previously described.[44] The *Z′* factor for the assay reported herein is 0.84 ± 0.03, confirming that it is suitable for HTS. We also studied how much DMSO the assay tolerates. At 10% DMSO the fluorescence intensity decreases about 50%. However, this still results in a large dynamic range between positive and negative compounds, enabling the discrimination of hits. The signal stability is

Table 2. Inhibition of $(A\beta_{16-37}Y_{20}K_{22}K_{24})_4$ and $A\beta_{1-40}$ fibril formation.

Classification[a]	Compd	$(A\beta_{16-37}Y_{20}K_{22}K_{24})_4$ IC_{50} [μM]	$A\beta_{1-40}$ IC_{50} [μM]
very strong	basic blue 41	0.36	1.4[31]
	curcumin	0.35	0.19[32]
			0.8[33]
	methyl yellow	0.34	1.5[31]
	myricetin	0.25	0.29[34]
			0.9[31]
	thionin	0.32	0.3[31]
strong	chlorazol black E	0.9	0.3[31]
	hemin chloride	1.8	0.1[31]
			0.4[35]
	NDGA	1.2	0.16[32]
	rifampicin	1.4	4.9[31]
			6[36]
medium	cholyl-LVFFA	10	<5[29]
	tetracycline	35	50[b],[37]
weak	2-amino-4-chlorophenol	100	30[c],[38]
	4,4′-dihydroxybenzophenone	100	ND
non-inhibitors	α-lipoic acid	>100	3.2[39]
			>100[d]
	β-cyclodextrin	>100	ND
	camphorsulfonic acid	>100	ND
	dopamine	>100	0.01[40]
			10–100[e],[41]
			10–100[d]
	nicotine	>100	10000[42]
			>50[f],[43]
	pyridine	>100	>100000[42]

[a] Compounds are classified according to their inhibitory effect on the system $(A\beta_{16-37}Y_{20}K_{22}K_{24})_4$. [b] Determined in a study of $A\beta_{1-42}$ (220 μM). [c] $[A\beta_{1-42}]=7$ μM. [d] Determined in this study. [e] $[A\beta_{1-40}]=230$ μM. [f] Determined in a CD study of $A\beta_{1-42}$ (50 μM). ND = not determined.

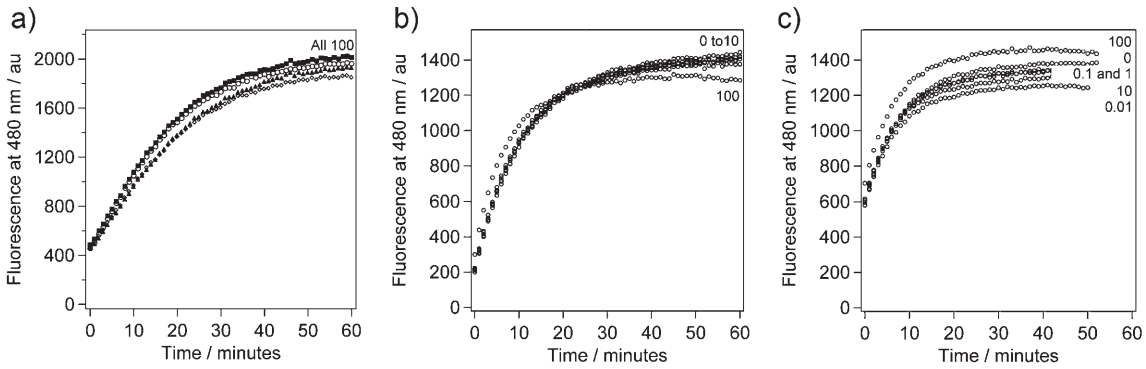

Figure 4. Kinetics data from non-inhibitors of $(A\beta_{16-37}Y_{20}K_{22}K_{24})_4$ fibril formation: a) pyridine (■), nicotine (○), β-cyclodextrin (▲), and camphorsulfonic acid (◇); b) α-lipoic acid; c) dopamine. Studies were performed as described in Figure 3, and respective inhibitor concentrations (μM) are indicated next to each curve.

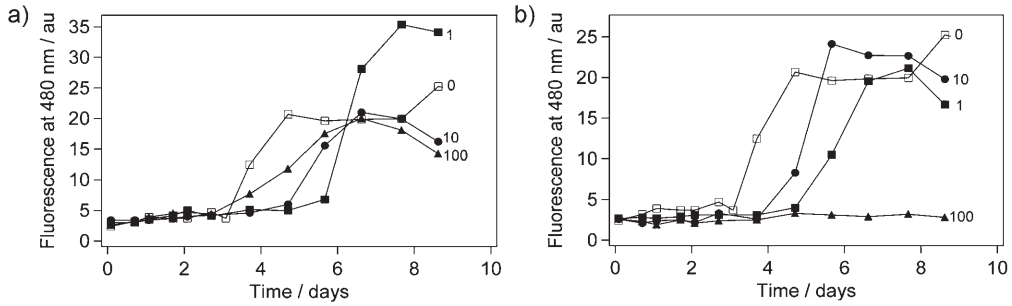

Figure 5. Control inhibition studies of $A\beta_{1-40}$ (50 μM) with a) α-lipoic acid and b) dopamine. Aggregation of $A\beta_{1-40}$ was performed in stagnant solution with HPO_4^{2-} (50 mM, pH 7.4) and NaCl (100 mM) at 37 °C; respective inhibitor concentrations (μM) are indicated next to each curve. Data were obtained from 4-μL aliquots that were removed from the aggregation mixture and analyzed separately with a solution of ThT (96 μL, 10 μM) and HPO_4^{2-} (50 mM, pH 7.1).

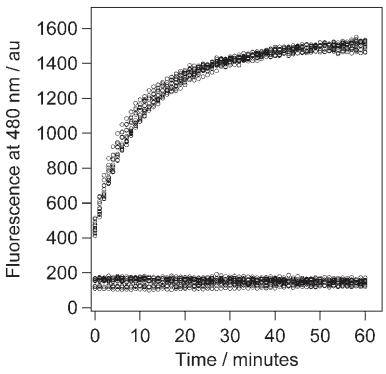

Figure 6. Determination of the Z' factor value for the fibril inhibitor screening tool. In each of three individual 96-well plates, 12 controls with no inhibitor and 12 controls with curcumin (100 μM) were used for estimating the Z' value. The assays were performed as described in Figure 3. Here we show the results from one of the plates: the data at top represent the controls with no inhibitor and the data at bottom represent the controls with curcumin; the mean fluorescence values are 1496 ± 67 and 148 ± 14 au, respectively. See the Supporting Information for details from all three plates.

also good: after 24 hours there was no notable change in signal intensity of uninhibited or inhibited samples.

Discussion

The aggregation and formation of fibrils from Aβ is widely accepted to be a key factor in the development of Alzheimer's disease (AD). However, neither the cytotoxic mechanisms nor which aggregation state of Aβ exerts toxicity are well understood. The toxicity may come from unstructured assemblies during the nucleation phase, fibrils, amyloid, or combinations of these. Consequently, an important therapeutic approach in the prevention and control of AD are compounds that inhibit Aβ aggregation.

Herein we present a tool based on Aβ for high-throughput screening of amyloid inhibitor compounds. We show that the engineered fibril building block, $(A\beta_{16-37}Y_{20}K_{22}K_{24})_4$, is highly sensitive to a broad range of reported inhibitor molecules of Aβ fibril formation. This screening tool shows a number of advantages over native $A\beta_{1-40}$ for in vitro studies. These include fast controllable kinetics, no uncontrolled aggregation of stock peptide (as is the case for $A\beta_{1-40}$), highly reproducible data, and good signal stability, with a Z' factor of 0.84 ± 0.03, confirming its suitability for HTS.[44] Our system is easy to handle: to a solution of $(A\beta_{16-37}Y_{20}K_{22}K_{24})_4$ and ThT reporter we just add potential inhibitor molecules and then start the formation of fibrils by adding HPO_4^{2-}. Using 96-well microplates, a total volume of 70 μL was used in each study, and the concentration of the $(A\beta_{16-37}Y_{20}K_{22}K_{24})_4$ assembly was only 4 μM; concentrations of $A\beta_{1-40}$ between 50 and 230 μM are commonly required

for in vitro screening studies.[32,39–42] The kinetics were monitored by following the change in fluorescence of ThT–fibril interactions in real time, data were collected at 1-min intervals, and all kinetics were complete within one hour, as compared with $A\beta_{1-40}$, which can take days under the same conditions. An additional advantage of the $(A\beta_{16-37}Y_{20}K_{22}K_{24})_4$ assembly is the improvement in the ThT fluorescence signal-to-noise ratio, which is easily observed by comparing Figure 2a with Figure 2c. In Figure 2a we observe 4 μM $(A\beta_{16-37}Y_{20}K_{22}K_{24})_4$ with a fluorescence maximum (F_{max}) of 650 arbitrary units (au), and in Figure 2c we observe 2 μM $A\beta_{1-40}$ with $F_{max}=20$ au, yet ThT was present at 10 μM in both cases, and identical instrumentation was used. We expect this difference to be due to the high solubility of $(A\beta_{16-37}Y_{20}K_{22}K_{24})_4$, but could also result from differences in the number of binding sites or in the quantum yield of fluorescence.

The aim of these studies was to prove our system as a rapid screening tool of Aβ inhibitors. We studied 19 different compounds composed of well-known inhibitors of Aβ aggregation as well as non-inhibitors. All the compounds tested showed a high degree of correlation with in vitro inhibition studies of $A\beta_{1-40}$, and inhibited the aggregation of $(A\beta_{16-37}Y_{20}K_{22}K_{24})_4$ in a dose-dependent fashion. From the group of compounds we classified as very strong inhibitors, myricetin was the strongest, with an IC_{50} value of 0.25 μM. This is followed by thionin, methyl yellow, curcumin, and basic blue 41, all with IC_{50} values below 0.4 μM. The natural products myricetin, a wine-related polyphenol, and the yellow curry pigment curcumin are also potent antioxidants, making them highly interesting as drug candidates as well as lead molecules for the development of drugs against AD.

Compounds we classified as strong inhibitors are, with the strongest compound first, chlorazol black E ($IC_{50}=0.9$ μM), NDGA ($IC_{50}=1.2$ μM), rifampicin ($IC_{50}=1.4$ μM), and hemin chloride ($IC_{50}=1.8$ μM). The IC_{50} values obtained with $(A\beta_{16-37}Y_{20}K_{22}K_{24})_4$ are all in good agreement with the respective in vitro values obtained with studies on $A\beta_{1-40}$. This group of important inhibitors includes the natural product NDGA, which is isolated from the creosote bush, *Larrea tridentata*,[45] and is a potent oxygen radical scavenger.[46] Also in this group, rifampicin is a semisynthetic antibiotic and its mechanism of inhibition of Aβ toxicity is suggested to involve the scavenging of hydroxyl radicals[36] and/or binding to Aβ through hydrophobic interactions, thus inhibiting its aggregation.[47]

The groups of medium and weak inhibitors include the modified Aβ fragment cholyl-LVFFA, the inhibitor tetracycline, 2-amino-4-chlorophenol, and 4,4′-dihydroxybenzophenone. For our system these inhibitors show IC_{50} values that lie between 10 and 100 μM, similar to the values obtained from $A\beta_{1-40}$. Cholyl-LVFFA is a so-called β-sheet breaker peptide and is different from the other compounds tested, as it uses the important recognition sequence, LVFFA, of Aβ to bind to the growing fibrils, and the bulky cholyl group disrupts and dissociates them.[29]

The validity of our system was also tested by using compounds reported to have small effects on Aβ fibril formation. We first tested dopamine, nicotine, and pyridine, which have been reported to have IC_{50} values of about 100 μM, 10 mM, and >100 mM, respectively, for native Aβ. The corresponding IC_{50} values obtained from $(A\beta_{16-37}Y_{20}K_{22}K_{24})_4$ were all in good correlation with those previously reported, giving IC_{50} values >100 μM. Our results with dopamine are thus in good agreement to those reported by the research group of Fink[41] and our current control study with $A\beta_{1-40}$. In contrast to these results, Yamada and co-workers[40] recently reported an IC_{50} value of 0.01 μM for dopamine under similar experimental conditions as those presented herein. The only experimental difference is the pretreatment and storage of $A\beta_{1-40}$: Whereas the Yamada's research group dissolved the peptide in 0.02% ammonia solution and stored it at −80 °C, we pretreated $A\beta_{1-40}$ with hexafluoroisopropanol (HFIP), resolubilized the lyophilized product in distilled water, removed eventual aggregates by centrifugation, and stored it at −20 °C. Notably, Fink and co-workers studied a higher concentration of $A\beta_{1-40}$ (230 μM) in Tris (25 mM) and NaCl (100 mM) at pH 7.4, as compared with our studies and those of the Yamada research group, with $A\beta_{1-40}$ (50 μM) in HPO_4^{2-} (50 mM) and NaCl (100 mM) at pH 7.4. Therefore, an explanation for this discrepancy should not be due to different experimental conditions, as we used the same as those reported by Yamada and co-workers. Instead, it may be, as indicated by Fink, that an oxidative product or products of dopamine, formed at pH >5, were found to be more active for inhibition of fibril formation of α-synuclein.[41] It should be noted that the degradation of compounds in our HTS assay is kept to a minimum owing to the fast kinetics that are performed at room temperature.

Thereafter we tested the nonaromatic compounds β-cyclodextrin and camphorsulfonic acid; aromatic structure is commonly found in Aβ aggregation inhibitors. Both of these compounds showed IC_{50} values >100 μM as was expected. Interestingly, the compound β-cyclodextrin has previously been shown to diminish the neurotoxic effects of an $A\beta_{1-40}$ cell line, but any destabilization effect on $A\beta_{1-40}$ fibril formation has not been demonstrated.[48]

The only compound that did not show a corresponding inhibitory profile against $(A\beta_{16-37}Y_{20}K_{22}K_{24})_4$ as reported against $A\beta_{1-40}$ fibril formation is the nonaromatic lipid-soluble antioxidant α-lipoic acid, for which Yamada and co-workers recently published an IC_{50} value of 3.2 μM.[39] In our studies we found that α-lipoic acid is a non-inhibitor against $(A\beta_{16-37}Y_{20}K_{22}K_{24})_4$. Under identical experimental conditions as those reported by the Yamada group, we studied the inhibition of $A\beta_{1-40}$ fibril formation with α-lipoic acid, and we did not observe inhibition as previously reported. In our studies of $A\beta_{1-40}$ fibril inhibition we observed fibril formation at all concentrations of α-lipoic acid studied, thus giving an IC_{50} value >100 μM, as is the case for the $(A\beta_{16-37}Y_{20}K_{22}K_{24})_4$ system. An explanation for this discrepancy may be, as suggested above for dopamine, that degradation products of α-lipoic acid could be more active for inhibition of fibril formation. Therefore, the inhibition studies presented herein demonstrate that fibril formation with the engineered building block $(A\beta_{16-37}Y_{20}K_{22}K_{24})_4$ behaves identically to $A\beta_{1-40}$ fibril formation.

Is our system relevant for the study of Aβ fibril inhibitors?

The formation of fibrils with $(A\beta_{16-37}Y_{20}K_{22}K_{24})_4$ occurs only through hydrophobic (side-chain) and backbone hydrogen bonding (cross-β-sheet) interactions. Both of these interactions direct the growth and create highly stable fibrils. The Aβ sequence in our engineered fibril building block was reduced to residues 16–37 of the full-length Aβ peptide, and thus contains only the highly ordered β-strand segments of Aβ (Figure 1).[19] An important attribute of the residue 16–37 sequence is that it retains the intra-peptide antiparallel β-sheet as well as the parallel inter-peptide β-sheet interactions, which shorter peptides lack. As the $(A\beta_{16-37}Y_{20}K_{22}K_{24})_4$ construct contains only the β-sheet-forming segment of Aβ, the ability to stop fibril formation or to destabilize this region could only be performed with potential Aβ inhibitor drugs.

The segment $A\beta_{1-15}$ was previously determined to be an unstructured region in the folded Aβ fibril and is thus not important for its stability,[19] which is also the reason we deleted it from our fibril building block. On the other hand, the segment $A\beta_{1-15}$ may have implications for the initial formation of fibrils, and drugs that target this segment would therefore have potential in the prevention of AD. However, such a strategy of targeting molecules to this segment seems highly unpractical, as it implies that at an early stage, patients would likely be continuously exposed to relatively high concentrations of the drug. In principle, such a drug would increase the lag phase of fibril formation. Furthermore, if fibrils are present or formed, drugs that target this unstructured region of Aβ would have little effect on the continued growth of the fibrils.

The segment containing residues 25–35 of Aβ has been widely studied owing to its similar biological behavior to native Aβ. The fragment $A\beta_{25-35}$ is able to form fibrils and shows neurotoxicity in many studies.[49,50] Also, an IC_{50} value of 10 μM was determined from inhibition studies of fibril formation with curcumin; this inhibition is about 10-fold weaker than found for $A\beta_{1-40}$.[51] As the segment $A\beta_{25-35}$ is conserved in our model fibril building block together with the structural features described above, we believe our system contains all the important residues of Aβ fibril stability and thus serves as a good model for inhibitor screening.

There are a number of mechanisms that may cause decreased fluorescence of the reporter molecule ThT in inhibition studies of amyloid fibrils without affecting fibril structure, which are rarely discussed. One mechanism is quenching of ThT fluorescence. To avoid quenching, many researchers perform fluorescence measurements on highly diluted samples of the fibril-forming mixture. This is misleading, as quenching by energy transfer is distance dependant; usually a distance less than 6 nm (Förster radius) is required for notable quenching interactions between two compounds. Other quenching interactions require even shorter distances between probe and quencher. Indeed, unbound ThT is not observed in the fluorescence study, and thus dilution of the reaction mixture will not affect the quenching of fibril-bound inhibitor to fibril-bound ThT. In other words, only compounds that bind to fibrils can quench fibril-bound ThT, which is the probe studied.

Another mechanism of decreased fluorescence may be competitive binding to the fibrils between ThT and the compounds studied. In any case, if it is quenching, competitive binding, or fibril inhibition that decreases ThT fluorescence, all these mechanisms indicate binding of the compound to the fibril and are thus potential leads for the development of drugs against AD-associated fibril formation, as well as diagnostic compounds. For these reasons, the HTS system presented herein, as for other fluorescence-based systems, is intended primarily for inhibitor screening. Hits will therefore require further complementary in vitro and in vivo analysis. A method to discriminate between true and false hits is to perform microscopy on the hit samples, such as AFM or TEM.

The fluorescence of the reporter ThT can be decreased, without interaction of another compound with the fibril, through filter effects at the excitation or emission wavelengths. This could occur when the compounds have strong absorbencies at these wavelengths. To examine if this was possible with the compounds in our library, we analyzed their UV/Vis spectra. From this analysis we found that only curcumin, methyl yellow, chlorazol black E, and rifampicin have absorbencies near one or both of the excitation/emission wavelengths. For these four compounds we expect that, to some degree, the fluorescence decrease observed at high compound concentration is due to an absorbency filtration effect. However, the possibility that the decrease in fluorescence is entirely due to this effect can be excluded, as a strong decrease in fluorescence is still observed at very low compound concentrations, such as 1 μM, at which any filtration effect is negligible.

Speculating on the throughput potential of this system, we expect that in the environment of HTS, thousands of compounds could be screened per day. As the end fluorescence values are the most relevant data, only one measurement per plate is required. In other words, the plate would be screened one hour after its preparation. As a measurement takes less than one minute for a 96-well plate, many plates could be measured in a single day.

Conclusions

The simplicity of this assay system and its rapid folding kinetics makes it highly interesting to screen large numbers of compounds to generate novel hits for Aβ fibril formation inhibitors; this is currently underway in our laboratory. The simplicity lies in the fact that our HTS tool produces data that are easily interpreted, as the assay has a high Z' factor of 0.84 ± 0.03. Difficulties encountered in screening for inhibitors of native Aβ are: poor signal-to-noise ratio, slow folding kinetics, and the fact that the kinetics of the same sample studied in different wells often show different lag phases and end fluorescence values. Together, these problems have been hurdles for HTS researchers. For comparison, we studied our system with a broad range of reported inhibitors and non-inhibitors, and found good correlation to previously reported results with in vitro inhibition studies on native Aβ. For these reasons, we expect that this screening tool will be highly advantageous for the rapid search of Aβ fibril inhibitors.

Experimental Section

Materials

Synthetic $(A\beta_{16-37}Y_{20}K_{22}K_{24})_4$ was prepared as previously described.[28] Cholyl-LVFFA was prepared as previously described.[29] All inhibitor compounds were purchased from Sigma except myricetin, which was obtained from Fluka. All other reagents were of the highest analytical grade available.

Preparation of $A\beta_{1-40}$

$A\beta_{1-40}$ was synthesized on an Applied Biosystems 433A peptide synthesizer using an Fmoc-Val-Novasyn-TGA resin (Novabiochem) with a substitution level of 0.24 mmol. Amino acids were coupled at a 10-fold excess under HBTU/DIPEA activation (HBTU = *O*-(benzotriazol-1-yl)-*N*,*N*,*N*′,*N*′-tetramethyluronium hexafluorophosphate, DIPEA = *N*,*N*-diisopropylethylamine). Coupling times of 60 min were used, and difficult residues were double coupled. Deprotection and cleavage from the resin was carried out with a mixture of TFA/TIS/H_2O/EDT (94:2:2:2 *v*/*v*), 15 mL (g resin)$^{-1}$, with occasional swirling for 2 h (TFA = trifluoroacetic acid, TIS = triisopropylsilane, EDT = 1,2-ethanedithiol). After filtration and reduction of the TFA by N_2 bubbling, the peptide was precipitated and washed three times with cold Et_2O. Purification was performed by reversed-phase HPLC on a semi-preparative C5 Discovery Wide Pore (Supelco) with a gradient of 9→90% CH_3CN over 30 min, with 0.1% TFA and a flow rate of 6 mL min^{-1}. The retention time of $A\beta_{1-40}$ was 14 min. The purity was >95% by analytical RP HPLC. The identity was verified by ESMS: the calculated weight for $A\beta_{1-40}$ is 4328 Da; found 4328.8 Da $[M+H]^+$. $A\beta_{1-40}$ was lyophilized and stored at −20 °C.

Preparation of $A\beta_{1-40}$ peptide stock solution

For aggregation assays, a stock solution of $A\beta_{1-40}$ was prepared as follows: 2.7 mg was dissolved in 200 μL of 1,1,1,3,3,3-hexafluoro-2-propanol (HFIP) to disassemble preformed aggregates, and thereafter it was lyophilized. Pure H_2O was then added, and the solution was centrifuged at 12000 *g* to remove eventual aggregates. The stock solution was divided into portions and stored at −20 °C until use. The stock concentration of $A\beta_{1-40}$ was regarded as 500 μM.

Preparation of $(A\beta_{16-37}Y_{20}K_{22}K_{24})_4$ peptide stock solutions

For aggregation assays, a stock solution of $(A\beta_{16-37}Y_{20}K_{22}K_{24})_4$ was prepared as follows: 0.24 mg was dissolved in 150 μL HFIP/H_2O (1:1) and lyophilized. Thereafter the peptide was dissolved in pure H_2O (1.2 mL). Stock peptide concentrations were determined spectrophotometrically using an extinction coefficient of 9160 cm^{-1} M^{-1} at $\lambda = 280$ nm.[28] The stock concentration of $(A\beta_{16-37}Y_{20}K_{22}K_{24})_4$ was 20 μM, and storage was at −20 °C until use.

Preparation of inhibitor stock solutions

Inhibitors were dissolved in EtOH if possible; hemin chloride was dissolved in MeOH, otherwise DMSO was used. Stock solutions of 10 mM were first prepared, and thereafter they were diluted into EtOH/H_2O (1:1) or DMSO/H_2O (1:1) with the following concentrations: 5000, 500, 50, 5, and 0.5 μM. Final concentrations of EtOH or DMSO in inhibition studies were 1%. Dopamine and α-lipoic acid were dissolved with DMSO for the inhibition studies with $A\beta_{1-40}$.

Measurement of $A\beta_{1-40}$ aggregation

Aggregation of $A\beta_{1-40}$ was performed in 96-well black polypropylene microplates (Geriner). To each well an aliquot of the peptide stock solution was mixed into the aggregation buffer to give a final composition of $A\beta_{1-40}$ (50 μM), sodium phosphate (50 mM), and NaCl (100 mM) pH 7.4. Thereafter 2-μL aliquots of the inhibitors were added. Microplates were sealed with a plastic sheet and incubated in a Molecular Devices Spectra MAX Gemini XS microplate reader at 37 °C. Data were obtained from 4-μL aliquots that were removed from the aggregation mixture and analyzed separately with 96 μL of a solution of ThT (10 μM) and HPO_4^{2-} (50 mM) pH 7.1. Kinetics of aggregation were monitored in an PerkinElmer Luminescence Spectrometer LS50 by following the increase in ThT fluorescence using a 0.3-cm reduced quartz cuvette with excitation at 440 nm and collecting data from 460 to 600 nm. Slits for excitation and emission were 2.5 and 10 nm, respectively. Kinetic data of $A\beta_{1-40}$ were fitted with the stretched exponential function:

$$F_t = F_\infty - \Delta F^{-(kt)^n}$$

for which F_t is the fluorescence at time t, F_∞ is the fluorescence after complete fibril formation, ΔF is the difference in fluorescence between t_0 and t_∞, k is the rate constant, and values greater than 1 for the parameter n indicate a sigmoidal transition with an initial lag phase.[52]

Measurement of $(A\beta_{16-37}Y_{20}K_{22}K_{24})_4$ aggregation

ThT was added to the stock solution of $(A\beta_{16-37}Y_{20}K_{22}K_{24})_4$. Aliquots (48.6 μL) of the $(A\beta_{16-37}Y_{20}K_{22}K_{24})_4$/ThT mixture were put into the required wells of 96-well black polypropylene microplates. Inhibitors were then added (1.4 μL), and the solution in each well was mixed with the addition of 20 μL stock phosphate buffer solution (17.5 mM) to give a total volume of 70 μL. The final concentrations obtained were 4 μM $(A\beta_{16-37}Y_{20}K_{22}K_{24})_4$, 10 μM ThT, and 5 mM HPO_4^{2-}. The concentrations of studied inhibitors were 0, 0.01, 0.1, 1, 10, and 100 μM. Microplates were analyzed in a Molecular Devices Spectra MAX Gemini XS microplate spectrophotometer at ambient temperatures. Measurements of ThT binding were started immediately by recording the fluorescence at 1-min intervals using band-pass filters of 440 nm for excitation, 480 nm for emission, and a cut-off filter of 455 nm. In this procedure ThT fluorescence is measured throughout the assembly process in real time. The IC_{50} values were calculated from the fluorescence values obtained at the end of the kinetics studies, that is, the value at 60 min. These values were then plotted against the log of the inhibitor concentration. Fitting the data with a sigmoidal function in Igor Pro software (WaveMetrics), the IC_{50} was obtained at the fluorescence halfway point.

Evaluation of the HTS tool

The $(A\beta_{16-37}Y_{20}K_{22}K_{24})_4$-based assay was evaluated for its Z' factor according to Zhang et al.[44] under the same conditions used for the aggregation measurement of $(A\beta_{16-37}Y_{20}K_{22}K_{24})_4$. This involved three distinct 96-well plates, each containing 12 positive wells in the presence of the inhibitor curcumin (100 μM) and 12 control wells in the absence of inhibitors. DMSO was used in this study at a concentration of 1%.

Acknowledgements

This work was supported by grants from AFM-INSERM GIS "maladies rares amyloses héréditaires" (no. AE02013 KSA), IUF, and ACI.

Keywords: Alzheimer's disease · amyloid β peptides · high-throughput screening · inhibitors · protein folding

[1] P. T. Lansbury, Jr., *Proc. Natl. Acad. Sci. USA* **1999**, *96*, 3342 – 3344.
[2] R. M. Murphy, *Annu. Rev. Biomed. Eng.* **2002**, *4*, 155 – 174.
[3] C. M. Dobson, *Semin. Cell Dev. Biol.* **2004**, *15*, 3 – 16.
[4] G. G. Glenner, C. W. Wong, *Biochem. Biophys. Res. Commun.* **1984**, *120*, 885 – 890.
[5] C. Haass, D. J. Selkoe, *Cell* **1993**, *75*, 1039 – 1042.
[6] J. T. Jarrett, E. P. Berger, P. T. Lansbury, Jr., *Biochemistry* **1993**, *32*, 4693 – 4697.
[7] J. T. Jarrett, J. Lansbury, T. Peter, *Cell* **1993**, *73*, 1055 – 1058.
[8] M. P. Mattson, *Nature* **2004**, *430*, 631 – 639.
[9] M. P. Mattson, B. Cheng, D. Davis, K. Bryant, I. Lieberburg, R. E. Rydel, *J. Neurosci.* **1992**, *12*, 376 – 389.
[10] N. Arispe, E. Rojas, H. B. Pollard, *Proc. Natl. Acad. Sci. USA* **1993**, *90*, 567 – 571.
[11] Z. Galdzicki, R. Fukuyama, K. C. Wadhwani, S. I. Rapoport, G. Ehrenstein, *Brain Res.* **1994**, *646*, 332 – 336.
[12] A. Demuro, E. Mina, R. Kayed, S. C. Milton, I. Parker, C. G. Glabe, *J. Biol. Chem.* **2005**, *280*, 17294 – 17300.
[13] W. E. Muller, S. Koch, A. Eckert, H. Hartmann, K. Scheuer, *Brain Res.* **1995**, *674*, 133 – 136.
[14] R. P. Mason, J. D. Estermyer, J. F. Kelly, P. E. Mason, *Biochem. Biophys. Res. Commun.* **1996**, *222*, 78 – 82.
[15] A. Ferreira, Q. Lu, L. Orecchio, K. S. Kosik, *Mol. Cell. Neurosci.* **1997**, *9*, 220 – 234.
[16] X. Huang, C. S. Atwood, M. A. Hartshorn, G. Multhaup, L. E. Goldstein, R. C. Scarpa, M. P. Cuajungco, D. N. Gray, J. Lim, R. D. Moir, R. E. Tanzi, A. I. Bush, *Biochemistry* **1999**, *38*, 7609 – 7616.
[17] M. A. Smith, C. A. Rottkamp, A. Nunomura, A. K. Raina, G. Perry, *Biochim. Biophys. Acta* **2000**, *1502*, 139 – 144.
[18] J. P. Blass, *J. Neurosci. Res.* **2001**, *66*, 851 – 856.
[19] R. Tycko, *Curr. Opin. Struct. Biol.* **2004**, *14*, 96 – 103.
[20] I. Dewachter, F. Van Leuven, *Lancet Neurol.* **2002**, *1*, 409 – 416.
[21] D. Schenk, R. Barbour, W. Dunn, G. Gordon, H. Grajeda, T. Guido, K. Hu, J. Huang, K. Johnson-Wood, K. Khan, D. Kholodenko, M. Lee, Z. Liao, I. Lieberburg, R. Motter, L. Mutter, F. Soriano, G. Shopp, N. Vasquez, C. Vandevert, S. Walker, M. Wogulis, T. Yednock, D. Games, P. Seubert, *Nature* **1999**, *400*, 173 – 177.
[22] M. A. Findeis, *Biochim. Biophys. Acta* **2000**, *1502*, 76 – 84.
[23] F. E. Cohen, J. W. Kelly, *Nature* **2003**, *426*, 905 – 909.
[24] A. Lorenzo, B. A. Yankner, *Proc. Natl. Acad. Sci. USA* **1994**, *91*, 12243 – 12247.
[25] H. LeVine III, *Methods Enzymol.* **1999**, *309*, 274 – 284.
[26] H. LeVine III, *Protein Sci.* **1993**, *2*, 404 – 410.
[27] R. J. Chalifour, R. W. McLaughlin, L. Lavoie, C. Morissette, N. Tremblay, M. Boule, P. Sarazin, D. Stea, D. Lacombe, P. Tremblay, F. Gervais, *J. Biol. Chem.* **2003**, *278*, 34874 – 34881.
[28] G. T. Dolphin, P. Dumy, J. Garcia, *Angew. Chem.* **2006**, *118*, 2765 – 2768; *Angew. Chem. Int. Ed.* **2006**, *45*, 2699 – 2702.
[29] M. A. Findeis, G. M. Musso, C. C. Arico-Muendel, H. W. Benjamin, A. M. Hundal, J.-J. Lee, J. Chin, M. Kelley, J. Wakefield, N. J. Hayward, S. M. Molineaux, *Biochemistry* **1999**, *38*, 6791 – 6800.
[30] Y. Porat, A. Abramowitz, E. Gazit, *Chem. Biol. Drug Des.* **2006**, *67*, 27 – 37.
[31] S. Taniguchi, N. Suzuki, M. Masuda, S.-i. Hisanaga, T. Iwatsubo, M. Goedert, M. Hasegawa, *J. Biol. Chem.* **2005**, *280*, 7614 – 7623.
[32] K. Ono, K. Hasegawa, H. Naiki, M. Yamada, *J. Neurosci. Res.* **2004**, *75*, 742 – 750.
[33] F. Yang, G. P. Lim, A. N. Begum, O. J. Ubeda, M. R. Simmons, S. S. Ambegaokar, P. P. Chen, R. Kayed, C. G. Glabe, S. A. Frautschy, G. M. Cole, *J. Biol. Chem.* **2005**, *280*, 5892 – 5901.
[34] K. Ono, Y. Yoshiike, A. Takashima, K. Hasegawa, H. Naiki, M. Yamada, *J. Neurochem.* **2003**, *87*, 172 – 181.
[35] D. Howlett, P. Cutler, S. Heales, P. Camilleri, *FEBS Lett.* **1997**, *417*, 249 – 251.
[36] T. Tomiyama, A. Shoji, K.-i. Kataoka, Y. Suwa, S. Asano, H. Kaneko, N. Endo, *J. Biol. Chem.* **1996**, *271*, 6839 – 6844.
[37] G. Forloni, L. Colombo, L. Girola, F. Tagliavini, M. Salmona, *FEBS Lett.* **2001**, *487*, 404 – 407.
[38] F. G. De Felice, M. N. N. Vieira, L. M. Saraiva, J. D. Figueroa-Villar, J. Garcia-Abreu, R. Liu, L. Chang, W. L. Klein, S. T. Ferreira, *FASEB J.* **2004**, *18*, 1366 – 1372.
[39] K. Ono, M. Hirohata, M. Yamada, *Biochem. Biophys. Res. Commun.* **2006**, *341*, 1046 – 1052.
[40] K. Ono, K. Hasegawa, H. Naiki, M. Yamada, *Neurochem. Int.* **2006**, *48*, 275 – 285.
[41] J. Li, M. Zhu, A. B. Manning-Bog, D. A. Di Monte, A. L. Fink, *FASEB J.* **2004**, *18*, 962 – 964.
[42] K. Ono, K. Hasegawa, M. Yamada, H. Naiki, *Biol. Psychiatry* **2002**, *52*, 880 – 886.
[43] A. R. Salomon, K. J. Marcinowski, R. P. Friedland, M. G. Zagorski, *Biochemistry* **1996**, *35*, 13568 – 13578.
[44] J.-H. Zhang, T. D. Y. Chung, K. R. Oldenburg, *J. Biomol. Screening* **1999**, *4*, 67 – 73.
[45] J. Luo, T. Chuang, J. Cheung, J. Quan, J. Tsai, C. Sullivan, R. F. Hector, M. J. Reed, K. Meszaros, S. R. King, T. J. Carlson, G. M. Reaven, *Eur. J. Pharmacol.* **1998**, *346*, 77 – 79.
[46] Y. Goodman, M. R. Steiner, S. M. Steiner, M. P. Mattson, *Brain Res.* **1994**, *654*, 171 – 176.
[47] T. Tomiyama, S. Asano, Y. Suwa, T. Morita, K.-i. Kataoka, H. Mori, N. Endo, *Biochem. Biophys. Res. Commun.* **1994**, *204*, 76 – 83.
[48] P. Camilleri, N. J. Haskins, D. R. Howlett, *FEBS Lett.* **1994**, *341*, 256 – 258.
[49] J. Xu, S. Chen, S. H. Ahmed, H. Chen, G. Ku, M. P. Goldberg, C. Y. Hsu, *J. Neurosci.* **2001**, *21*, RC118.
[50] C. J. Pike, D. Burdick, A. J. Walencewicz, C. G. Glabe, C. W. Cotman, *J. Neurosci.* **1993**, *13*, 1676 – 1687.
[51] C. Riviere, T. Richard, L. Quentin, S. Krisa, J.-M. Merillon, J.-P. Monti, *Bioorg. Med. Chem.* **2007**, *15*, 1160 – 1167.
[52] S. S. S. Wang, Y.-T. Chen, P.-H. Chen, K.-N. Liu, *Biochem. Eng. J.* **2006**, *29*, 129 – 138.

Received: May 3, 2007
Revised: July 2, 2007
Published online on September 17, 2007

